AVS JVSTB Journal of Vacuum Science & Technology B

Advanced electrical imaging of dislocations in Mg–In-codoped GaN films

Sy-Hann Chen, Sheng-Ping Hou, J. H. Hsieh, F. C. Chang, and W. K. Chen

Citation: Journal of Vacuum Science & Technology B **24**, 108 (2006); doi: 10.1116/1.2150223
View online: http://dx.doi.org/10.1116/1.2150223
View Table of Contents: http://scitation.aip.org/content/avs/journal/jvstb/24/1?ver=pdfcov
Published by the AVS: Science & Technology of Materials, Interfaces, and Processing

Articles you may be interested in
Dislocation movement in GaN films
Appl. Phys. Lett. **97**, 261907 (2010); 10.1063/1.3532965

On the origin of threading dislocations in GaN films
J. Appl. Phys. **106**, 073513 (2009); 10.1063/1.3225920

Defect reduction in nonpolar a -plane GaN films using in situ Si N x nanomask
Appl. Phys. Lett. **89**, 041903 (2006); 10.1063/1.2234841

Dislocation reduction in GaN thin films via lateral overgrowth from trenches
Appl. Phys. Lett. **75**, 2062 (1999); 10.1063/1.124916

Dislocation mediated surface morphology of GaN
J. Appl. Phys. **85**, 6470 (1999); 10.1063/1.370150

Re-register for Table of Content Alerts

Create a profile.

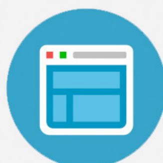

Sign up today!

Redistribution subject to AVS license or copyright; see http://scitation.aip.org/termsconditions. Download to IP: 140.113.38.11 On: Thu, 01 May 2014 02:35:21

Advanced electrical imaging of dislocations in Mg–In-codoped GaN films

Sy-Hann Chen[a)]
Department of Applied Physics, National Chiayi University, Chiayi 600, Taiwan, Republic of China

Sheng-Ping Hou and J. H. Hsieh
Department of Materials Engineering, Mingchi University of Technology, Taishan, Taipei Hsien 243, Taiwan, Republic of China

F. C. Chang and W. K. Chen
Department of Electrophysics, National Chiao-Tung University, Hsin Chu 300, Taiwan, Republic of China

(Received 5 August 2005; accepted 7 November 2005; published 12 January 2006)

Conducting atomic force microscopy and scanning surface-potential microscopy have been applied to image the surfaces of Mg–In-codoped GaN films grown by low-pressure metal-organic chemical-vapor deposition. Biscyclopentadienylmagnesium (CP_2Mg) and trimethylindium (TMIn) have been used as the codoping sources in the experiment. The dislocation density at the film surface reduces to the lowest level ($\sim 1.0 \times 10^9$ cm^{-2}) when the TMIn/CP_2Mg flow rate ratio is about 1. The dislocation density tends to rise when the flow ratio increases, and carriers of the film accumulate near the rim of the dislocation at an accelerated speed. The work function of dislocation is also found lower than that of nondislocation areas. Such electrical unevenness may seriously influence the light emission of the component, which should not be ignored during fabrication and deserves careful attention. © *2006 American Vacuum Society.* [DOI: 10.1116/1.2150223]

I. INTRODUCTION

GaN (Ref. 1) is now one of the most prominent semiconductor materials. Its direct energy gap (Eg) is 3.4 eV; in a hybrid crystal with InN or AlN, the Eg can be adjusted to a value between 1.9 and 6.3 eV. This has been the subject of intensive research for both optoelectronic and high-power microwave applications in recent years. The basic structure of GaN's light-emitting diode (LED) and laser diode (LD) optical elements is a *p*-*n* junction made by *n*-type and *p*-type GaN semiconductors. In GaN's LED, for achieving high lighting efficiency, the *n*-type GaN needs high electron concentration before electrons are injected into *p*-type GaN for recombination and lighting. To make the *n*-type and the *p*-type GaN semiconductors of high carrier concentrations, it is common to have GaN film undergo doping during growth. As GaN is more like an *n*-type semiconductor itself, the research at this stage tends to aim at how to make a *p*-type GaN of high stability.

In the research of *p*-type GaN, Mg, so far, is the only element used for doping for GaN. In 1989, Amano *et al.*[2] made a *p*-type GaN using low-energy electron-beam irradiation (LEEBI) after doping with Mg. During the growth of GaN, because of the stress and the inter-reaction caused by the incompatible lattice structure with the substrate, and the uneven distribution of dopant in the film, crystal dislocations[3–5] is created. With quantum confined effect, the electric charge builds up rapidly, creating significant impacts on the function and efficiency of the elements. In the present research, the electrical measurements of *p*-type GaN after doping can only be carried out on a broad view basis. That is, only average readings can be obtained, which grossly neglects the impact of the physical characteristics caused by the variation of regional profile. In our experiment, the atomic force microscopy (AFM) was first used to measure and compute the dislocation densities in Mg–In-codoped GaN films. Secondly, the conducting atomic force microscopy[6–12] (C-AFM) and scanning surface-potential microscopy[13–19] (SSPM) were applied to image surfaces' electricity of Mg–In-codoped GaN films over dislocations. The nanoscale imaging does allow us to learn better about the lighting system of GaN semiconductor, which is constructive and useful when it comes to improving the fabrication processes components.

II. EXPERIMENTAL SETUP AND SAMPLE DESCRIPTION

Experiments were performed under ambient conditions using a commercial AFM (Dimension 3100, Digital Instruments). Rectangular Si tips (CSC12, NT-MDT, Russia) with a spring constant of 1.75 N/m and resonant frequency of 155 kHz were used for these measurements. The tips were precoated with a Cr layer, provided by the manufacturer, and subsequently coated with a 10 nm Au film by ion sputtering.

The C-AFM procedures employed in our studies have been described previously.[6–8] In brief, a conductive tip is used in contact mode AFM scanning for simultaneous topography and current measurements. A positive bias voltage is applied to the sample through electronics in the AFM while the tip is grounded. The current through the tip is measured with a current amplifier and is recorded as a function of tip position. The resulting current images show nonuniformities in sample conductivity.

[a)]Author to whom correspondence should be addressed; electronic mail: shchen@mail.ncyu.edu.tw

Redistribution subject to AVS license or copyright; see http://scitation.aip.org/termsconditions. Download to IP: 140.113.38.11 On: Thu, 01 May 2014 02:35:21

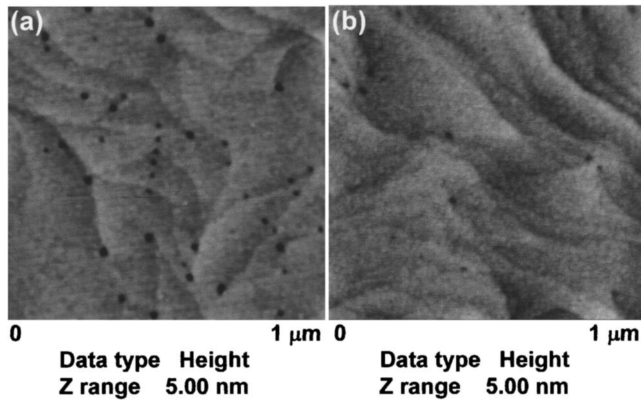

FIG. 1. AFM images of *p*-type GaN films (a) with CP_2Mg flow rate of 250 SCCM and (b) with CP_2Mg and TMIn flow rates of 250 SCCM.

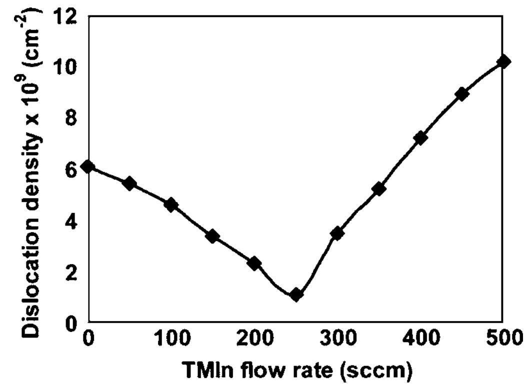

FIG. 2. Dislocation densities of Mg–In-codoped GaN films as a function of In source flow rate.

The SSPM is used to image variations in contact potential difference (CPD) $\Delta\Phi$ between a conducting AFM tip and sample. The CPD is given by

$$\Delta\Phi = \frac{\Phi_{\text{tip}} - \Phi_{p\text{-GaN}}}{e}, \quad (1)$$

where Φ_{tip} and $\Phi_{p\text{-GaN}}$ are the work functions (WF) of the tip and sample, respectively, and e is the magnitude of the electron charge. To acquire AFM and CPD images, a topographic line scan is first obtained by tapping mode AFM imaging, and then the tip traces over the same line at a lift height from sample surface. During this "lift-mode" scan, ac voltage with a dc offset is applied to the conducting AFM tip. The ac voltage frequency is set to resonant cantilever-free vibration frequency. The oscillation amplitude of the cantilever is zeroed by adjusting the external dc voltage until it matches the surface potential. The required dc voltage follows the localized contact potential of the surface and is recorded by the computer with reversing sign. The CPD images, which can be related to changes in the sample's surface Fermi-level position, are thereby obtained. The basic principles of SSPM have been described in detail elsewhere.[13–19]

The samples used in this study were fabricated by a low-pressure metal-organic chemical-vapor deposition (LP-MOCVD). A 0.3 μm low-temperature GaN nucleation layer was first deposited on a 2 in. sapphire (0001) substrate at 520 °C followed by $\sim$2 μm of Mg–In-codoped *p*-type GaN grown at 1110 °C. Electronic grade trimethylgallium (TMGa), ammonia (NH_3), biscyclopentadienylmagnesium (CP_2Mg), and trimethylindium (TMIn) were used as the Ga, N, Mg, and In source precursors, respectively. In an attempt to investigate the isoelectronic effect of In on the *p*-type GaN, a series of samples were prepared by using constant CP_2Mg flow rate of 250 SCCM (standard cubic centimeter per minute) (25.5 μmol/min) and various TMIn flow rates from 0 to 500 SCCM (0 to 0.590 μmol/min).

III. RESULTS AND DISCUSSION

Results and data of the experiment are stated and discussed hereunder in three parts. Firstly, surfaces of the specimens were scanned using AFM and the change of dislocation density was analyzed. Secondly and thirdly, current and CPD images of the film surface were then analyzed using C-AFM and SSPM, respectively, to conduct analysis on local electrical conductivity and work functions.

A. Dislocation densities

Images of the surface appearances without and with In doping are shown in Figs. 1(a) and 1(b), respectively. The scanned area was 1×1 μm^2 and the dislocation pits can be observed on both micrographs. For the In-doped sample, the In precursor flow rate was set at 250 SCCM. Through calculation, it is found that the dislocation density changed from 4.0×10^9 to 1.0×10^9 cm^{-2} when the sample was doped with In.

Figure 2 shows that the dislocation densities vary with the change of In doping concentration. Ten different areas were picked from each specimen for AFM scanning to obtain an average dislocation density. As shown in the figure, dislocation density drops dramatically when TMIn flow rate increases from 0 to 250 SCCM, while it tends to increase as TMIn flow rate is greater than 250 SCCM, or when $TMIn/CP_2Mg$ flow rate ratio is greater than 1. Reasons are as follows: Mg atom is smaller than Ga atom so that interspaces between atoms in a lattice become uneven during the deposition process in which Ga atoms are replaced by Mg atoms followed by the increase of dislocation densities. In the case of In codoping, In is bigger than Ga which may offset the size difference between Mg and Ga after codoping. Consequently, interspaces in the lattice become more uniformed and dislocation densities are reduced. Still, concentration of In atoms should be controlled carefully below a certain limit. Otherwise, Ga atoms being replaced in considerable quantities may lead to crush between atoms. This is the main reason why dislocation densities rise dramatically when TMIn flow rate is greater than 250 SCCM. In addition, cross-sectional analysis reveals that the size of dislocation ranges from 20 to 80 nm, while the depth is between 2 and 8 nm. No regular pattern exists in the distribution, and no correlation has been observed between dislocation size and TMIn flow rate.

Redistribution subject to AVS license or copyright; see http://scitation.aip.org/termsconditions. Download to IP: 140.113.38.11 On: Thu, 01 May 2014 02:35:21

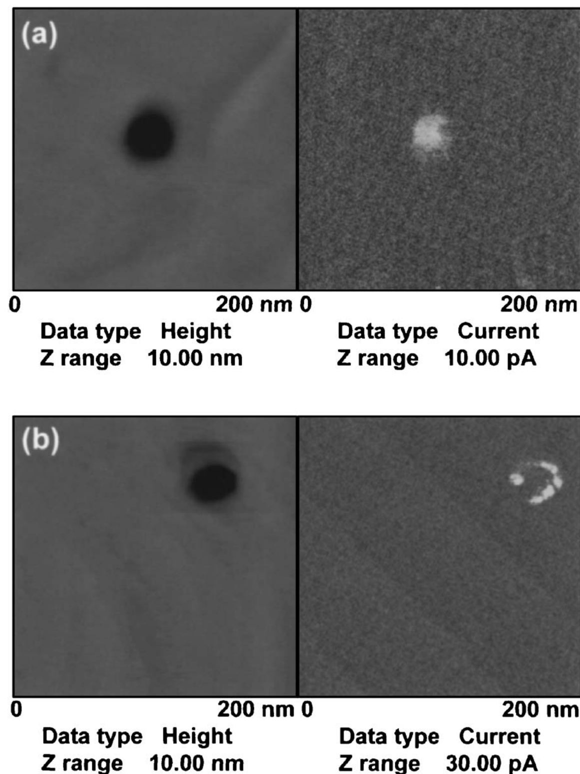

FIG. 3. Topography (left) and current (right) images of *p*-type GaN films (a) with CP_2Mg flow rate of 250 SCCM and (b) with CP_2Mg and TMIn flow rates of 250 SCCM.

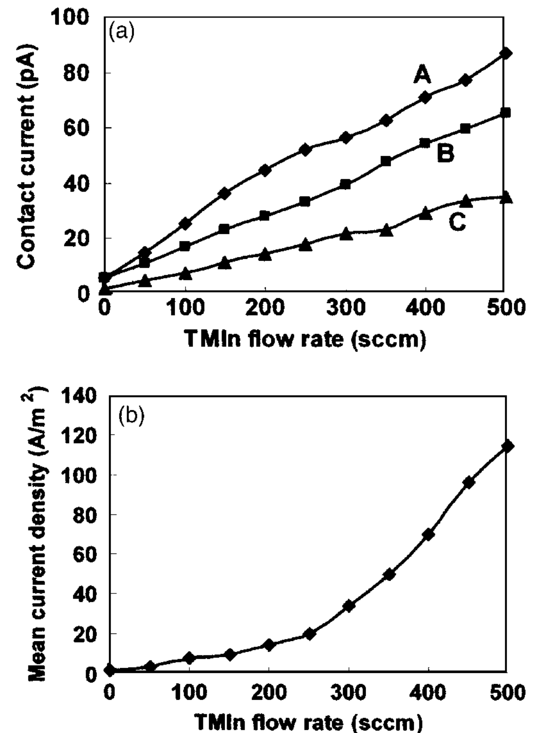

FIG. 4. Variations of (a) contact currents inside dislocation (■), at smooth areas (▲) and near the dislocation rim (♦), and (b) mean current density of Mg–In-codoped GaN films as a function of TMIn flow rate.

B. Conductive features

Topography (left) and current (right) images of the Mg-doped and Mg–In-codoped (TMIn flow rate=250 SCCM) GaN films measured at contact mode with a positive bias of 7 V on samples are shown in Figs. 3(a) and 3(b), respectively. According to the results presented in Ref. 20, carrier concentration of Mg–In-codoped GaN is higher than that of Mg-doped GaN. The overall conductivity of the former, therefore, is bound to be better. The mean contact currents are 2.12 and 20.12 pA for Mg-doped and Mg–In-codoped samples. Nevertheless, the fact worthy of further investigation is that additional carriers from Mg–In codoping are not evenly distributed over the film surface but may form localized accumulation. It can be clearly seen from the figure that the distribution of contact current inside dislocation is more uniform in Mg-doped sample, which has a mean current of 5.51 pA, while, for Mg–In-codoped sample, it rises to about 33.24 pA and has uneven distribution. Particularly, the maximum contact current near the rim reaches 52.12 pA. Mean contact currents without and with In doping at smooth areas (without dislocation) are 1.66 and 18.11 pA, respectively.

Figure 4(a) shows the change of contact currents at three localized areas as a function of TMIn flow rates. Contact currents inside dislocation (curve B) and at smooth areas (curve C) exhibit a tendency of progressive increase along with the increase of In-doping concentration. The largest gradient is obtained from the dislocation core, particularly near the dislocation rim (curve A) where carriers seriously accumulate. Such area of high conductivity is formed by quantum confined effect yet with lower breakdown voltage which tends to result in leakage currents of components under normal operation. For electronic components, these are the most vulnerable areas to overheating. Figure 4(b) displays the correlation between mean current densities and TMIn flow rate. The mean current density here is calculated from a C-AFM scanning area of $1 \times 1\ \mu m^2$. The result implies that the mean current density of *p*-type GaN goes up abruptly when the flow rate ratio of $TMIn/CP_2Mg$ is greater than 1. Based on the analysis stated above, such high rise of current density should result from the increase of dislocation number and does not benefit component efficacy.

C. Work function distributions

The CPD mapping was made in the lift mode at a lift scan height (tip-sample separation) of 30 nm with 5 V ac voltage applied to the tip. The measurement was obtained simultaneously with the topography scan in the tapping mode using an electrically Cr/Au-coated tip. The topography (left) and CPD (right) images of the Mg-doped and Mg–In-codoped (TMIn flow rate=250 SCCM) GaN films in a $200 \times 200\ nm^2$ scanning area are shown in Figs. 5(a) and 5(b), respectively. The dc offset values for the right side images in Figs. 5(a) and 5(b), which were measured across a cross section of the CPD images before the flatten analysis, are 0.30 and 0.17 V, respectively. Because the WF of the gold-coated probe was 5.10 ± 0.03 eV, calibrated using a highly oriented pyrolytic graphite (HOPG) substrate,[21] the mean

Redistribution subject to AVS license or copyright; see http://scitation.aip.org/termsconditions. Download to IP: 140.113.38.11 On: Thu, 01 May 2014 02:35:21

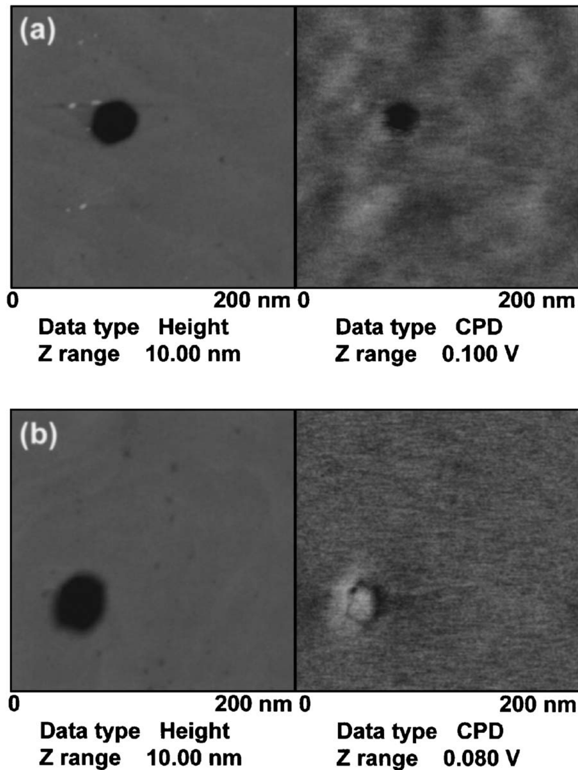

FIG. 5. Topography (left) and CPD (right) images of p-type GaN films (a) with CP_2Mg flow rate of 250 SCCM and (b) with CP_2Mg and TMIn flow rates of 250 SCCM. The CPD images have been dealt with flatten analysis.

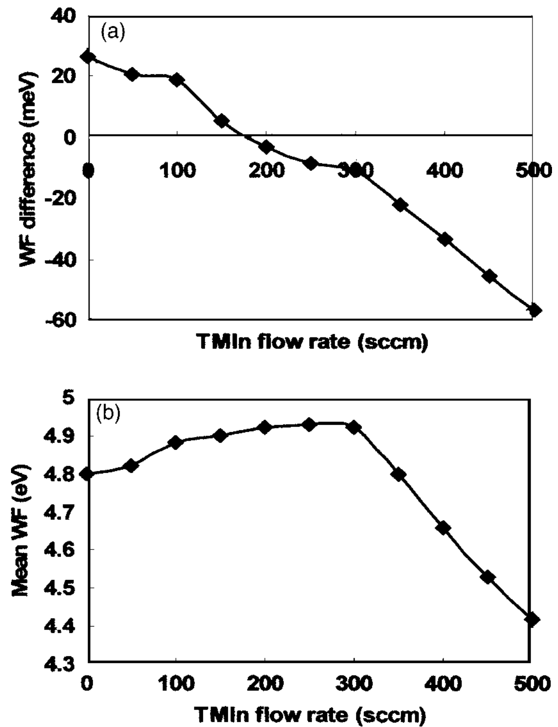

FIG. 6. Variations in (a) single dislocation WF difference and (b) mean WF of Mg–In-codoped GaN films as a function of TMIn flow rate.

WF values of the two samples were calculated to be 4.80 and 4.93 eV, respectively, by using Eq. (1). From such analysis we come to realize that doping In atoms will help increase the mean WF of p-type GaN. However, further observation of dislocations on CPD images reveals that CPD is lower than the mean by 0.026 V without In doping [Fig. 5(a)] and the WF is 4.80+0.026 eV. After In doping [Fig. 5(b)], CPD becomes higher than the mean by 0.008 V and the WF is 4.93−0.008 eV. This means that, after In doping, WF in the dislocation is less progressively efficient when compared with the nondislocation area nearby.

Figure 6(a) represents the variation of WF difference of a dislocation (in contrast to mean WF) as a function of TMIn flow rate. After TMIn flow rate is greater than 180 SCCM, the difference between the dislocation WF and the overall WF enlarges gradually as TMIn flow rate increases. This phenomenon, together with the increase in the number of dislocation (as discussed in Sec. I), intensifies the impact on the mean WF. The variation of mean WF (measured by SSPM scanning of a 1×1 μm^2 area) as a function of TMIn flow rate is shown in Fig. 6(b). The number of dislocation decreases and WF difference narrows when TMIn flow rate is between 100 and 300 SCCM, which has limited impact on the overall mean WF. However, dislocation densities increase dramatically and WF difference expands when TMIn flow rate is greater than 300 SCCM, which leads to an abrupt drop of mean WF.

In LD or LED components, the wavelength of luminescence relies solely on the energy gap, which is the WF difference between n-type and p-type GaN. As a result, the change of p-type GaN implies a shift of wavelength in the luminescence of components. In this experiment, the increase of In concentration leads to a drop of mean WF of p-type GaN, which, based on the assumption of fixed WF of n-type GaN, results in the expansion of energy gap and shorter wavelength of luminescence radiated. To fabricate LD or LED luminescence components with shorter wavelengths is one of the emphases in current studies. Although this can be achieved by increasing the concentration of doping In, based on the discussion in Sec. II, carriers will accumulate at dislocation areas in considerable quantities when it exceeds the critical doping concentration (TMIn flow rate >300), which shortens the lifetime of components and shadows with negative effects.

IV. CONCLUSION

To sum up, when compared with traditional optoelectronic detecting techniques, C-AFM and SSPM are known for their high resolution, which provides accurate and microscopic electrical detecting data for optoelectronic films such as GaN, and can be used as a tool for fabricating process improvement. A conclusion can be drawn from the above discussion that In doping with proper concentration, that is, to control $TMIn/CP_2Mg$ flow rate ratio at about 1, will have three benefits to local surface electrical features of p-type GaN film: (1) to reduce surface dislocation density, (2) to increase carrier concentration, and (3) to make surface WF

Redistribution subject to AVS license or copyright; see http://scitation.aip.org/termsconditions. Download to IP: 140.113.38.11 On: Thu, 01 May 2014 02:35:21

uniform. However, when TMIn/CP_2Mg flow rate ratio is greater than 1.2, carriers may accumulate on around dislocation cores in considerable quantities and induce local electrical variation to the film surface, which will then cause negative effects on luminescence efficacy of components.

[1]H. P. Maruska and J. J. Tietjen, Appl. Phys. Lett. **15**, 327 (1969).
[2]H. Amano, M. Kito, K. Hiramatsu, and I. Akasaki, Jpn. J. Appl. Phys., Part 2 **28**, L2112 (1989).
[3]H. M. Ng, D. Doppalapudi, T. D. Moustakas, N. G. Weimann, and L. F. Eastman, Appl. Phys. Lett. **73**, 821 (1998).
[4]M. Iwaya, T. Takeuchi, S. Yamaguchi, C. Wetzel, H. Amano, and I. Akasaki, Jpn. J. Appl. Phys., Part 2 **37**, L316 (1998).
[5]J. W. Hsu, M. J. Manfra, R. J. Molnar, B. Heying, and J. S. Speck, Appl. Phys. Lett. **81**, 79 (2002).
[6]H.-N. Lin, S.-H. Chen, Y.-Z. Lee, and S.-A. Chen, J. Appl. Phys. **89**, 3976 (2001).
[7]H.-N. Lin, S.-H. Chen, Y.-Z. Lee, and S.-A. Chen, J. Vac. Sci. Technol. B **19**, 308 (2001).
[8]H.-N. Lin, H.-L. Lin, S.-S. Wang, L.-S. Yu, G.-Y. Perng, S.-A. Chen, and S.-H. Chen, Appl. Phys. Lett. **81**, 2572 (2002).
[9]A. Bietsch, M. A. Schneider, M. E. Welland, and B. Michel, J. Vac. Sci. Technol. B **18**, 1160 (2000).
[10]T. W. Kelley and C. D. Fribie, J. Vac. Sci. Technol. B **18**, 632 (2000).
[11]L. Cai, H. Tabata, and T. Kawai, Nanotechnology **12**, 211 (2001).
[12]J. M. Mao, I. K. Sou, J. B. Xu, and I. H. Wilson, J. Vac. Sci. Technol. B **16**, 14 (1998).
[13]S.-H. Chen, J. Appl. Phys. **97**, 073713 (2005).
[14]H. O. Jacobs, P. Leuchtmann, O. J. Homan, and A. Stemmer, J. Appl. Phys. **84**, 1168 (1998).
[15]Y. Oyama, Y. Majima, and M. Iwamoto, J. Appl. Phys. **86**, 7087 (1999).
[16]L. Zhang, T. Sakai, N. Sakuma, and T. Ono, Jpn. J. Appl. Phys., Part 1 **39**, 3728 (2000).
[17]G. L'evêque, P. Girard, E. Skouri, and D. Yarekha, Appl. Surf. Sci. **157**, 251 (2000).
[18]B. Bhushan and A. V. Goldade, Appl. Surf. Sci. **157**, 373 (2000).
[19]S. Ono, M. Takeuchi, and T. Takahashi, Appl. Phys. Lett. **78**, 1086 (2001).
[20]F. C. Chang, K. C. Shen, H. M. Chung, M. C. Lee, W. H. Chen, and W. K. Chen, Chin. J. Phys. (Taipei) **40**, 637 (2002).
[21]It would be much better to use a freshly cleaved HOPG substrate, and perform a measurement on it before measuring the *p*-type GaN surfaces. HOPG has a fairly stable work function of about 4.6 eV in the ambient, so it can be used as a standard sample.

Redistribution subject to AVS license or copyright; see http://scitation.aip.org/termsconditions. Download to IP: 140.113.38.11 On: Thu, 01 May 2014 02:35:21